

Millimeter-Wave Interference Avoidance via Building-Aware Associations

Jeemin Kim, Jihong Park[†], Seunghwan Kim, Seong-Lyun Kim, Ki Won Sung[‡], and Kwang Soon Kim

Abstract—Signal occlusion by building blockages is a double-edged sword for the performance of millimeter-wave (mmW) communication networks. Buildings may dominantly attenuate the useful signals, especially when mmW base stations (BSs) are sparsely deployed compared to the building density. In the opposite BS deployment, buildings can block the undesired interference. To enjoy only the benefit, we propose a *building-aware association* scheme that adjusts the directional BS association bias of the user equipments (UEs), based on a given building density and the concentration of UE locations around the buildings. The association of each BS can thereby be biased: (i) toward the UEs located against buildings for avoiding interference to other UEs; or (ii) toward the UEs providing their maximum reference signal received powers (RSRPs). The proposed association scheme is optimized to maximize the downlink average data rate derived by stochastic geometry. Its effectiveness is validated by simulation using real building statistics.

Index Terms—Millimeter-wave communications, building blockages, base station association, load balancing, average data rate, stochastic geometry.

I. INTRODUCTION

The use of millimeter-wave (mmW) spectrum is a promising way to achieve the 1,000-fold capacity improvement in 5G cellular networks [1], [2]. It is envisaged to provide 20-100 times larger bandwidth, and thereby to resolve the spectrum crunch of the traditional cellular systems using the spectrum below 6 GHz carrier frequency. Utilizing such abundant mmW spectrum resource is however not free, but needs to pay a price for the significant distance attenuation induced by its vulnerability to signal blockages such as buildings and human bodies [3].

To compensate the severe distance loss of mmW signals, it is suitable to make the beam mainlobes sharpened and aligned toward the target directions [3]–[5]. Due to this strong signal directionality, mmW signals may rarely interfere with each other. Nevertheless, if interference occurs, its impact is detrimental [6]. The mmW beam directions should therefore be carefully decided in order to avoid significant interference.

Motivated by this, in this paper we seek a design for deciding the interference-avoiding mmW beam directions in a downlink urban outdoor scenario. A straightforward solution can be made by using full interference channel information at each base station (BS). This, unfortunately, requires a massive number of channel information exchanges among all BSs in

a recursive manner [7]. Instead, we focus on the building density within the network region, compared to BS density. The buildings are obviously a major source of mmW signal blockages, and therefore the building density determines how much and how frequently mmW interference occurs. When building density is relatively high, both interfering probability and interference amount become negligibly small. Otherwise, it necessitates a sophisticated beam direction control to avoid interference.

In pursuit of avoiding mmW interference, we suggest a beam control idea making mmW beams steered toward buildings so as to maximize the downlink average data rate. The user equipments (UEs) in front of a building can thereby receive the desired signals, while less incurring interference to the UEs behind the building. Since the locations of UEs and buildings are random, the beam direction control is a challenging task. In fact, too much beam steering toward buildings may significantly increase the leakage of beams that interferes with the UEs adjacent to the buildings. Furthermore, the extreme beam steering may lead to no UEs associated within the beam directions and/or to increase the association distances, while unbalancing the association loads among BSs. These issues become more critical in an urban outdoor scenario where UEs are concentrated around buildings¹.

In this paper, we tackle these issues by proposing a *building-aware association* algorithm with a directional association bias $\beta \in [0, 1]$ that adjusts the beam steering amount toward buildings (see Fig. 1). The proposed design is operated based on the full knowledge of each BS's neighboring building locations and sizes, obtained via the map of the network area.

Specifically, if $\beta = 0$, i.e. a baseline without building-aware associations, each BS omni-directionally broadcasts a reference signal as in conventional LTE systems [11]. A BS allows the UE associations, ensuring the UEs' maximum average reference signal received powers (RSRPs). Such a BS is hereafter denoted as O-BS.

When $0 < \beta \leq 1$, with the proposed algorithm, some BSs only allow the associations of the UEs in front of their nearest buildings, hereafter denoted as D-BSs. A BS becomes D-BS if its mainlobe beam is not leaked to the sides of the nearest building, when the beam points at the center of the building. The rest of the BSs are set as O-BSs which keep allowing omni-directional UE associations (see Fig. 2(a)).

As β increases, the ratio of D-BS to O-BS increases. Here, if D-BSs broadcast the reference signals only in the fixed directions toward buildings, some UEs may not receive any

J. Kim, S. Kim, S.-L. Kim, and K. S. Kim are with the School of Electrical and Electronic Engineering, Yonsei University, Seoul, Korea (email: {jmkim,shkim}@ramo.yonsei.ac.kr, {slkim,ks.kim}@yonsei.ac.kr).

[†]J. Park is with the Department of Electronic Systems, Aalborg University, Denmark (email: jihong@es.aau.dk).

[‡]K. W. Sung is with Wireless@KTH, KTH Royal Institute of Technology, Kista, Sweden (e-mail: sungkw@kth.se).

¹People are likely to be gathered around the buildings around which sidewalks, bus stops, and cafe terraces are placed [8]–[10].

reference signals, stuck in the network coverage holes. To prevent this in the proposed algorithm, instead of a BS, each UE omnidirectionally broadcasts a reference signal if it does not receive any reference signal, and associates with the BS reporting the maximum RSRP out of all BSs. By so doing, every UE ensures its BS association.

Finally, β is optimized so as to maximize the average downloading rate of a randomly selected UE, i.e. a typical UE, while coping with the increases in association distances and load unbalancing due to the directional association biasing.

A. Related Works

The inter-BS beam coordination has a great potential to improve network capacity [4], [12]–[14]. In [12] and [13], the coordination algorithm where three adjacent BSs coordinate their beams has been investigated. However, in a real network, the amount of channel information sharing between cooperative BSs is limited due to the backhaul capacity. To reduce the backhaul burden, a centralized beam coordination has also been studied where the actions are decided by a central entity [14]. Although such a centralized scheme reduces the channel information exchange, its viability still relies on the latency of the exchanged information. Furthermore, in some network scenarios where the central entity is absent, e.g. spectrum sharing among different radio access technologies, such beam coordination cannot be utilized.

Traditionally, the blockage-vulnerable nature of mmW signals in most prior works has been interpreted as an obstacle to overcome [15], [16]. As a possible approach to tackle this issue, in [15], authors have proposed beam switching from a line-of-sight (LOS) link to a collection of non-LOS links when the LOS link breakage occurs. By utilizing a group of non-LOS links, BSs can bypass the obstacles. In [16], the multi-hop architecture is designed to compensate for the short LOS distance and to enhance the communication success probability. However, our study focuses on exploiting the blockage-vulnerable nature of mmW signals to filter network interference.

In addition, it is also worth mentioning that mmW communication is amenable to dense networks since BS densification can assure LOS conditions for more mmW transmissions, thereby relieving the severe distance attenuation problem [3]–[5], [17]. From this BS densification perspective, we expect that our algorithm will lead to network wide capacity improvements.

B. Contributions and Organizations

This paper proposes a *building-aware association* scheme to decrease the network interference in dense mmW networks by making BSs adjacent to buildings shape their beam signals toward the buildings. The main contributions of this paper are listed as follows:

- We proposed the building-aware association algorithm that mitigates mmW interference by exploiting the spatial information of buildings. The corresponding SIR coverage probability and average rate expressions are derived using stochastic geometry.

- We provided a spatial model of UE locations, capturing the user concentration around buildings.
- We optimized the directional association bias β of the proposed algorithm. For a special case when the ratio of BS density to UE density is extremely large, i.e. ultra-dense networks [5], we derived the closed-form optimal β . We thereby provided the design guideline: β should properly be increased to reduce more interference, as the density and sizes of buildings increase.
- We validated the effectiveness of the proposed association algorithm using real building geographic data. Compared to a traditional RSRP-based association, the proposed algorithm is always superior, and achieves higher average rate gains under lower building density locations.

The rest of the paper is organized as follows. The system model is specified in Section II. The SIR coverage and average rate in the building-aware association algorithm are derived in Section III. The results are used to derive the optimal bias β^* in Section IV. Numerical evaluation using real geometric data is presented in Section V. Finally, the concluding remarks are stated in Section V followed by the proofs of propositions and corollaries in the Appendix.

II. SYSTEM MODEL AND PROPOSED ASSOCIATION SCHEME

A. Network Model

We consider a dense mmW downlink cellular network where BSs, UEs, and buildings are densely located as in an urban outdoor hotspot. To reflect the randomness of the urban BS deployment, we assume the BS coordinates Φ_b follow a homogeneous Poisson Point Process (PPP) with density λ_b . We assume the urban buildings form a Boolean model of rectangles with average length d_l and width d_w , where $d_l > d_w$. The building center coordinates follow a homogeneous PPP Φ_ℓ with density λ_ℓ , independent of Φ_b .

We assume the LOS of each BS is guaranteed when its distance to a typical UE is within an average LOS distance R_L . Such distance is determined by the geography of building blockages, $R_L = \frac{\pi\sqrt{2}\exp(-\lambda_\ell d_l d_w)}{2\lambda_\ell(d_l+d_w)}$ [18]. Note that the deterministic LOS model provides an analytical simplicity, with only a minor gain in terms of SIR coverage compared with the random shape theory blockage model based result in a dense BS regime [19]. For simplicity, we neglect the effect of non-LOS signals², thus only BSs in the LOS region can transmit signals to a typical UE. We further consider that the LOS probabilities of different links are independent by ignoring the case in which a building blocks the links from neighboring BSs simultaneously [21]. The assumptions used in modeling the LOS links enables the analytical tractability, in return for reducing its accuracy. In section V, we validate that the effects of these assumptions are quite small through the simulation tests.

²Note that the effect of non-LOS links might be dominant in practice mmW communication due to the reflections [2], [18]. However, their channel gains are typically 20 dB weaker than the LOS channel gains [20]. Besides, in a dense network regime we are interested in, the mmW communication performance is highly limited by the LOS interferers, as verified in [21] through simulation tests. See [21] for the non-LOS link effects.

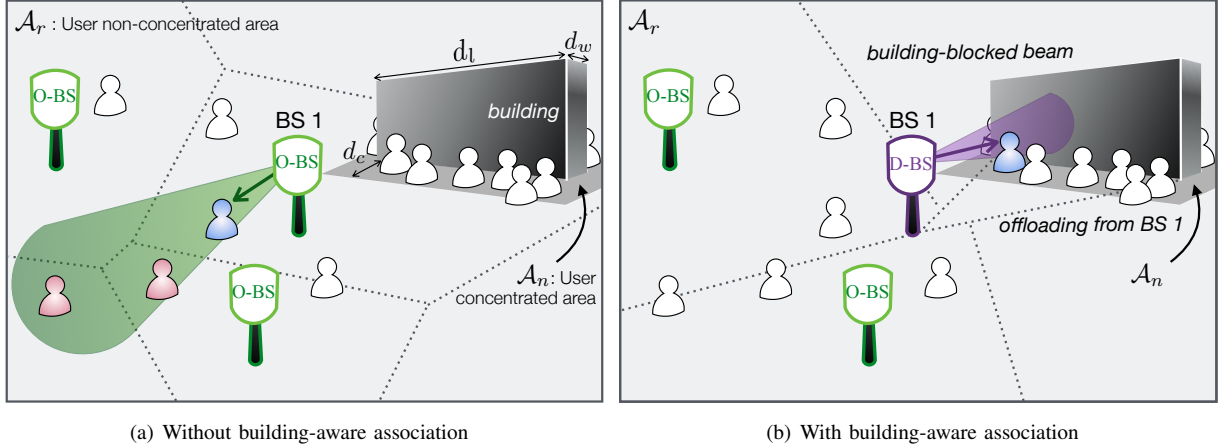


Fig. 1. Illustration of building-aware association algorithm in mmW cellular networks. UEs are concentrated around the buildings (compare \mathcal{A}_n with \mathcal{A}_r) whose average length and width are d_l and d_w , respectively. Without the building-aware association, a signal from BS 1 interferes with two UEs (see red UEs in (a)). Such inter-cell interference is removed by the aid of the proposed association which makes BS 1 transmit signals only toward UEs on the building side (D-BS); **Interference Decrement**. Furthermore, by shrinking the association areas of BS 1, traffic loads are balanced, i.e. the traffic load of D-BSs are offloaded to the BS transmitting signals in every directions (O-BS); **Load Balancing** (compare (a) with (b)).

B. UE Model

Consider an urban outdoor area where many UEs are concentrated around the buildings. We hereafter let U_n denote UEs located near the buildings, e.g., UEs sitting on a bench or a cafe terrace, or traveling along sidewalks. UEs that are not near the buildings are denoted by U_r . Indoor UEs are beyond the scope of this study since they do not cause interference with outdoor UEs, by considering that indoor and outdoor UEs utilize separate spectrum bands for communications or that even if they utilize the same spectrum, the transmitted signal cannot penetrate walls.

To establish criteria for determining whether UE is close to a building, we assume that each building has an area around it with a width of d_c as shown in Fig. 1. The UE in this area is regarded to be adjacent to the building. For clarity, let \mathcal{A}_n denote the area around the buildings, and the area excluding \mathcal{A}_n is denoted by \mathcal{A}_r . UE locations Φ follow a non-homogeneous PPP which are correlated with the building locations Φ_ℓ , and the corresponding areas \mathcal{A}_n and \mathcal{A}_r . The local intensity function of Φ has conditional intensity depending on the spatial location x [22], $\lambda(x) = \lambda_n \mathbb{1}_{x \in \mathcal{A}_n} + \lambda_r \mathbb{1}_{x \in \mathcal{A}_r}$, where $x \in \mathbb{R}^2$. The UE process Φ can be interpreted as a mixture of two homogeneous PPPs [23], i.e., when it is located in \mathcal{A}_n it follows PPP with density λ_n otherwise it follows PPP with density λ_r . The total integrated intensity $\int_{\mathbb{R}^2} \lambda(x) dx$ is denoted by λ .

To reflect the UE-concentration phenomenon, we let γ_c denote the user concentration ratio around buildings. The ratio is interpreted as i) the average time fraction that a typical UE is adjacent to a building, or ii) the average fraction of UE that is near buildings at a randomly chosen time. The UE densities λ_n and λ_r thus vary with the building parameters such as building density λ_ℓ or length d_l , and the user concentration ratio γ_c . In this study, we assume that the network can infer this concentration ratio by using UE location statistics such as the spatio-temporal congestion patterns resulting from the

daily routines [9].

Note that this non-homogeneous UE distribution does not prevent the use of PPP techniques such as Slyvnyak's theorem [24] required to analyze SIR, because it does not violate the isotropy in the transmitter point process (i.e. Φ_b).

C. Channel Model

To form directional beams, all BSs use analog beamforming implemented by utilizing phase shifters. Each BS steers the antenna direction of the antenna to achieve the maximum array gain at the associated UE. The error in angle estimation is ignored. For analytical tractability, the actual array pattern is approximated by a step function that quantizes the antenna array gains in binary form [19], [21], [25]. In this model, we assume the array gain within the half-power beamwidth θ radian is identical to the maximum power gain, denoted by g_m . The side lobe gain is denoted by g_s .

Each BS transmits a signal with unity power by utilizing the same frequency whose bandwidth is denoted by W . The transmitted signal experiences path-loss attenuation with the exponent $\alpha > 2$ and Rayleigh fading³ with unity mean, i.e. $h \sim \exp(1)$.

Hereafter, we only consider the network in an interference-limited regime, i.e. we neglect the noise power. Note that a mmW signal is more affected by noise power due to its wide communication bandwidth. Noise power elimination

³ Due to the blockage-vulnerability of mmW links, it is ideal to utilize different path loss exponents to the LOS and non-LOS links [19]. Since the LOS links are dominant to the mmW communication in a dense BS regime, we ignore non-LOS links as mentioned above. For the LOS links, the path loss exponent should be set close to 2 as discovered from channel measurement results [1], [30]. In addition, although the Rayleigh model may not fit well with the real mmW environment due to the LOS dependent mmW signals, this model can simplify the analytical expressions while providing a lower bound of the downlink rate under Nakagami fading, as mentioned in [5], [26], [27]. Simulation results have proved that using a Nakagami fading does not provide any additional design insights [28]. Furthermore, measurement shows that small-scale fading has a relatively little influence on the mmW communications [1], more relieving our concern to use the Rayleigh model.

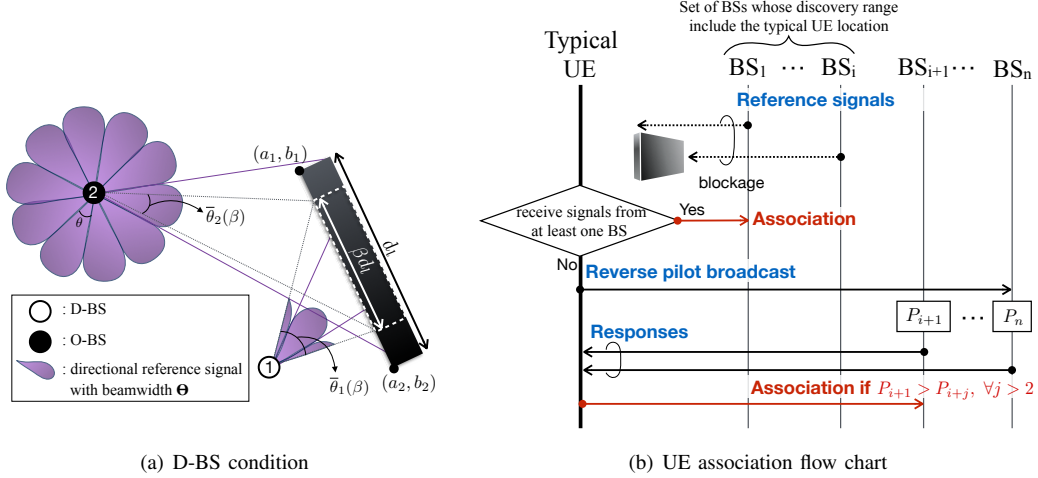


Fig. 2. Illustrations of building-aware association operations: **D-BS condition**. A BS becomes D-BS if its transmitted signal toward the nearest building does not leak beyond the building whose length is considered as βd_l , i.e. if $\theta < \bar{\theta}(\beta)$. Then BS 1 transmits the reference signal only toward the building with the discovery range $\bar{\theta}(\beta)$. **UE association**. Each BS transmits reference signal to its discovery range. When a typical UE receives at least one signal, it associates with the BS who gives the maximum power. If not, it broadcasts a pilot signal to discover the BS.

in this study, nevertheless, provides better tractability while being highly in accordance with the urban dense network scenario we are interested in. The effect of noise is numerically validated to be negligibly small in Section V.

Remember that our building-aware association scheme makes BSs adjacent to the buildings transmit signals only toward the buildings by shrinking their UE discovery ranges. Thus, a BS's signal interferes with a typical UE located at the origin o when the following two conditions hold: i) the distance to the typical UE is within the LOS distance R_L , and ii) the origin o is included in its discovery range. By using Slyvnyak's theorem [24], the SIR at a typical UE is

$$\text{SIR} := \frac{\mathbb{1}_{R_L}(|x_0|)g_m h|x_0|^{-\alpha}}{\sum_{x_i \in \Phi_b \setminus x_0} \mathbb{1}_{R_L}(|x_i|)G_i h_i |x_i|^{-\alpha}} \quad (1)$$

where $\mathbb{1}_{R_L}(r)$ is an indicator function which returns unity if $r \leq R_L$, x_0 and x_i for $i \in \{1, 2, \dots\}$ represent the association BS coordinates and the i -th nearest interfering BS coordinates, respectively. The notation $|\cdot|$ indicates the Euclidian norm. G_i means the directivity gain in the link from the i -th BS. The UE association rule is specified in the following section. Considering multiple associations at a BS, the BS selects a single UE per unit time slot using a uniformly random scheduler [29].

D. Building-aware UE Association

Within the building-aware association framework, every BS periodically transfers directional reference signals for UE association [31], but the discovery ranges of the BSs are not identical. We thus decompose the BSs into two types: BSs transmitting the reference signals in every direction (O-BSs); and BSs transmitting the signals only in the direction of a building (D-BSs). The specific building-aware association scheme follows the rules stated below:

1. **BS: Discovery Range Decision**. Assume every BS knows its location and the nearest building wall's two

vertices locations (see (a_1, b_1) and (a_2, b_2) in Fig. 2(a)). A BS becomes D-BS if its transmitted signal toward the nearest building does not leak beyond the building, whose length is considered as βd_l as shown in Fig. 2(a). Then the condition of a BS located at (x, y) is expressed as:

$$\theta \leq \bar{\theta}(\beta) = \left| \text{atan} \left[\frac{(1-\beta)b_2 + (1+\beta)b_1 - 2y}{(1-\beta)a_2 + (1+\beta)a_1 - 2x} \right] - \text{atan} \left[\frac{(1-\beta)b_1 + (1+\beta)b_2 - 2y}{(1-\beta)a_1 + (1+\beta)a_2 - 2x} \right] \right|. \quad (2)$$

The angle $\bar{\theta}(\beta)$ is utilized as the discovery range if the BS satisfies the above condition. Otherwise, its discovery range is 2π . As long as system parameters such as building density or beam width remain the same, the classification of a BS as a O-BS or a D-BS is maintained once it is determined.

2. BS-UE Association

- a) **Reference Signal Transmission**: Each BS transmits reference signals within the discovery range. When the transmitted signals meet a blockage, their signal strengths highly decrease before reaching to UE (see Fig. 2(b)).
- b) **BS Selection via Signal Strength Comparison**: UE listens for reference signals from BSs and transmits a connection request message to the BS that gives the maximum received power.
- c) **Reverse Pilot Broadcast**: If the UE detects a radio link failure or does not receive any reference signal, it sends a reverse pilot signal. BSs that receives the signal transmit their received power strengths to the UE, and the UE connects to a BS whose received power is the strongest.

The procedure 2 is periodically repeated to support UE handover or cell reselection. It is notable that the step 2-

c is to prevent our algorithm making coverage holes.⁴ This step resembles the Random Access (RA) procedure in Radio Resource Control (RRC) connection re-establishment in LTE [32]. Although this may incur additional control plane congestion, such case rarely happens especially in a dense network topology.

If $\beta = 0$, no BS satisfies the condition (2) and every BS transmits reference signals to UEs in every direction as in the RSRP-based association scheme. As β increases, the condition gives a loose constraint, increasing the number of D-BSs. At last when β becomes 1, all the BSs whose transmitted signals toward the nearest buildings do not leak beyond that building become a D-BS. The optimal bias for maximizing the average data rate is provided in the rest of this paper. It is worth mentioning that such association bias β is identically applied to all BSs even if the surrounding building characteristics of each BS are different. By so doing, the proposed algorithm obtains a one-shot solution and reduces the association decision time, yet in return for giving up finding the global optimal solution.

Note that with our algorithm, UE may regard that the building number is increased. This is because the buildings make their adjacent BSs transmit signals only to that building, so that they do not transmit main lobe signal to the UE on the opposite side of the building. From the UE viewpoint, it becomes as if the building obstacles increase. Thus in this study, we define the average distance from BS that can transmit main lobe signal as R_β (i.e. $R_\beta < R_L$), whose specific expression is derived in Section III.

III. COVERAGE AND RATE UNDER BUILDING-AWARE ASSOCIATION

The representation of mmW downlink rate using the building-aware association scheme is of prime concern in this section. The derived result will play a salient role in finding the rate-maximizing bias β in Section IV. In our building-aware association algorithm, a UE receives a distinct data rate according to several random variables such as signal distance, interfering BS locations, building locations, and cell coverage. The rate in this section thus represents the average data rate of a randomly picked UE considering these random variables.

A. SIR Coverage

We preliminarily represent the SIR coverage, defined as $P(\text{SIR} > t)$, in terms of the building-aware association bias β . To derive the SIR coverage, we utilize two approximations that are feasible under an urban dense mmW network regime: (i) *homogeneous main beam interferer thinning* with the thinning probability $\frac{\theta}{2\pi}$; and (ii) the *average LOS region*. Simulation results in Section V verifies the validity of each.

The first approximation tackles the non-homogeneity of the interfering BSs with the main lobe gain g_m . This mainly

results from the random UE selections in BSs which depend on the coverage areas of BSs and the non-uniformly distributed UE locations. In a dense network, however, the cell coverage area tends to be equal, diminishing the cell area dependency. Although this approximation gets loose as the non-homogeneity of the UE distribution is severe, we validate that the average main beam interfering probability of BSs is consistent with the thinning probability $\frac{\theta}{2\pi}$ when the concentration ratio is high through simulation experiments (see Fig. 3).

The second approximation is motivated by the average LOS ball model in [18]. From the perspective of a typical U_r , which is remote from the buildings, the LOS region is approximated to a ball area within an LOS distance R_L . On the other hand, from the perspective of a typical U_n , which is near a building, BSs located across the building cannot transmit any signals. Thus the average U_n LOS region becomes a half moon shape with a radius R_L as shown in Fig. 4(b). Hereafter we assume that a typical U_n is located at the center of the building wall and its distance to the building is negligible. This average LOS region model may reduce the analytical accuracy. However, since we consider the urban scenario where buildings are densely located, the difference between the actual and approximated LOS regions decreases, relieving this concern.

In the LOS region, D-BSs transmit signals toward the buildings, i.e. in the opposite direction of the typical UE located at the center of the LOS region (see Fig. 4). Such D-BSs transmit interfering signals only with the side lobe gain g_s . Thus, we define the average region of BSs that can transmit main lobe signals as follows, by considering the farthest distance from the building to the D-BS.

Lemma 1. In our algorithm, the maximum distance of D-BS from the building is $\frac{\beta d_l}{2 \tan(\frac{\theta}{2})}$. Therefore, the region of BSs that can transmit main lobe signals to a typical UE has a radius of $R_\beta = R_L - \frac{\beta d_l}{2 \tan(\frac{\theta}{2})}$.

Proof. See Appendix. ■

This result implies that for a typical U_n , distance R_β cannot be less than $\frac{R_L}{2}$. This is because, from the perspective of U_n , within the maximum distance of $\frac{\beta d_l}{2 \tan(\frac{\theta}{2})}$, there are D-BSs that transmit signals toward the U_n 's nearest building and interfere with the U_n (see Fig. 4(b)). Note that if a BS satisfies the D-BS condition for more than one building, the BS only transmits signals to the nearest building. That is, when a BS is closer than the maximum distance $\frac{\beta d_l}{2 \tan(\frac{\theta}{2})}$ not only from the building where the typical U_n is attached but also from the building at the edge of the average LOS region, i.e., $R_\beta < \frac{R_L}{2}$, the BS chooses the nearest building to transmit signals. Thus, the modified U_n LOS region no longer depends on β after the bias β increases to make $R_\beta = \frac{R_L}{2}$.

By considering the path-loss exponent of the LOS links is close to 2 and utilizing the above approximations and lemma, we can derive the SIR coverage as in the following proposition.

Proposition 1. (SIR Coverage) The SIR coverage of a typical

⁴When too many BSs associate with users in the building side (i.e., too many D-BSs), users far from buildings are likely to fail to find an associate BS. This might intensify the coverage hole problem in mmW system. To prevent this, we utilize the UE-centric association step 2-c.

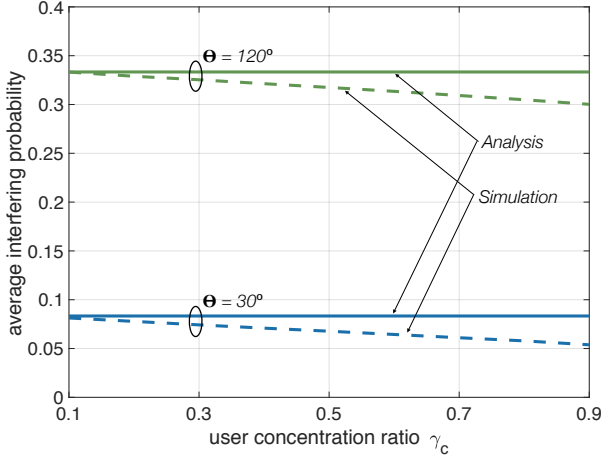


Fig. 3. Average main-lobe interfering probability of BSs according to the user concentration ratio γ_c and beam width θ ($\lambda = 400$ BSs/km², $\lambda_\ell = 400$ buildings/km², $d_l = 30$ m, $d_w = 10$ m, $t = 15$ dB).

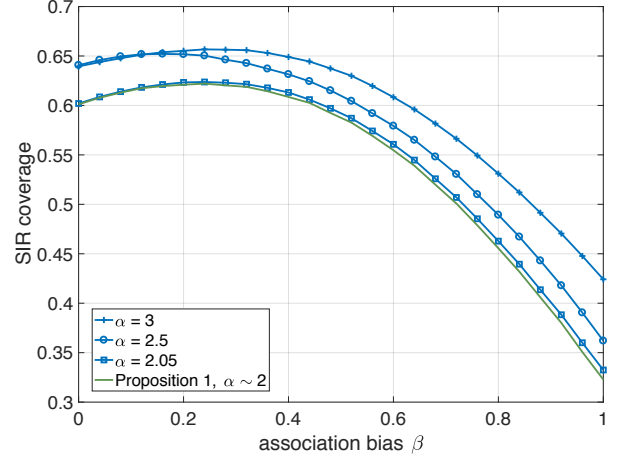


Fig. 5. SIR coverage according to the path-loss α ($\lambda_b = 400$ BSs/km², $\lambda_\ell = 400$ buildings/km², $\theta = \frac{\pi}{6}$ rad, $d_l = 30$ m, $d_w = 10$ m, $t = 10$ dB, $\gamma_c = 0.6$, $g_m = 20$ dB, $g_s = 0$ dB).

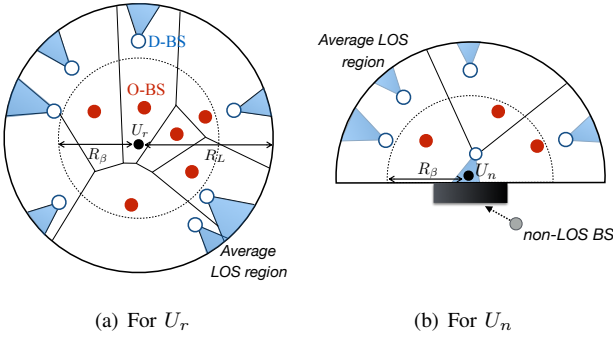


Fig. 4. Illustrations of the average LOS region and region of BSs that can interfere to a typical UE with a main lobe gain g_m .

UE becomes

$$\mathcal{S} = \gamma_c \mathcal{S}_n(\beta) + (1 - \gamma_c) \mathcal{S}_r(\beta), \quad (7)$$

where $\mathcal{S}_n(\beta)$ and $\mathcal{S}_r(\beta)$ represent the SIR coverage of a typical U_n and U_r , respectively. They are given as (3) and (4) at the bottom of the page.

Proof. See Appendix. ■

Note that one of key enablers to provide the SIR coverage is the assumption that the path-loss exponent α is equal to 2 since we mainly focus on the LoS links [30]. Fig. 5 shows that

the SIR coverage according to different α , verifying that the SIR coverage gap is small when α is larger than 2. Although such gap increases with α , they have similar tendencies.

The result shows that the association distance of a typical UE does not change with the bias β . This follows from the average LOS ball model in which the typical UE is located at the center of the LOS region (see Fig. 4). When the typical UE is U_r , its associated BS is located farthest from the buildings within the LOS ball region, i.e. it does not become a D-BS, maintaining the signal distance. When the typical UE is U_n , even if the associated BS becomes a D-BS, the connection is not cut off because the signal is transmitted toward the building to which the UE is attached. However, in actual networks the proposed algorithm might lengthen the UE association distances. This implies that the result in Proposition 1 deals with the upper-bound case from the signal strength perspective.

Note that the SIR coverages $\mathcal{S}_n(\beta)$ and $\mathcal{S}_r(\beta)$ have distinct tendencies according to the bias β . The following remark specifies these behaviors by considering two extreme cases.

Remark 1. If $\gamma_c = 0$, i.e. when UE is far from buildings at all times, the SIR coverage monotonically increases with β . If $\gamma_c = 1$, i.e. when UE is always near a building, the SIR coverage is convex-shaped over β .

This is mainly because, from the U_n perspective, a higher

$$\mathcal{S}_n(\beta) = F_0^{R_1} \left[1 + \ln \left(\frac{1+r_2}{1+t^{-1}} \right)^{P_\ell t} + \ln \left(\frac{1+r_1}{1+r_2} \right)^{p_a t} + \ln \left(\frac{1 + \frac{R_r^2}{r^2 t}}{1+r_1} \right)^{\frac{g_s t}{g_m}} \right] + F_{R_1}^{R_L} \left[1 + \ln \left(\frac{1+r_1}{1+t^{-1}} \right)^{p_a t} + \ln \left(\frac{1 + \frac{R_r^2}{r^2 t}}{1+r_1} \right)^{\frac{g_s t}{g_m}} \right] \quad (3)$$

$$\mathcal{S}_r(\beta) = 2F_0^{R_\beta} \left[2 + \ln \left(\frac{t+R_\beta^2 r^{-2}}{1+t} \right)^{2p_a t} + \ln \left(\frac{t+R_L^2 r^{-2}}{t+R_\beta^2 r^{-2}} \right)^{\frac{2g_s t}{g_m}} \right] + 2F_{R_\beta}^{R_L} \left[2 + \ln \left(\frac{t+R_L^2 r^{-2}}{t+1} \right)^{\frac{2g_s t}{g_m}} \right] \quad (4)$$

$$\text{where } F_a^b(x) = \int_a^b \pi \lambda_b r \exp\left(-\frac{\pi}{2} \lambda_b r^2 x\right) dr, \quad p_a = \frac{\theta}{2\pi} + \frac{2\pi - \theta}{2\pi} \left(\frac{g_s}{g_m} \right)^\alpha, \quad P_\ell = \left(\frac{(\pi - \theta)^2}{4 \sin^2(\theta)} + \frac{1}{4 \tan(\theta)} \right) \frac{8 \tan^2(\frac{\theta}{2})}{\pi} (1 - p_a) + p_a, \quad (5)$$

$$R_1 = \min \left(R_L - R_\beta, \frac{R_L}{2} \right), \quad r_1 = \max \left[\max \left(R_\beta, \frac{R_L}{2} \right)^2, r^2 \right] \left(r t^{\frac{1}{\alpha}} \right)^{-2}, \quad \text{and } r_2 = \min \left(R_L - R_\beta, \frac{R_L}{2} \right) \left(r t^{\frac{1}{\alpha}} \right)^{-2} \quad (6)$$

β makes more BSs transmit signals toward the buildings. In other words, high β decreases the LOS region (or R_β) while maintaining the signal strength. So the interference decreases. However, from the U_c perspective, the β increment firstly makes BSs located near buildings transmit signals in opposite directions from U_n and reduces its interference. When β is large, even BSs adjacent to U_n may become D-BSs and transmit signals toward the building to which U_n is attached. This incurs more interference to U_n . This finding helps not only to capture the impact of β in a more intuitive way, but also to find the optimal β^* which will be described in detail in Section IV.

B. Average Rate

We define the rate of a typical UE as $\mathcal{R} := E \left[\frac{W}{N+1} \right] P(\text{SIR} > t) \log[1+t]$, where W represents the bandwidth and N the UE number at a BS that associates with a typical UE. The SIR coverage in the previous section enables the determination of the average spectral efficiency $P[\text{SIR} > t] \log(1+t)$. To derive the rate \mathcal{R} , in addition, we need to calculate the available amount of bandwidth under the uniformly random scheduler, $\frac{W}{1+N}$. The random variable N , the UE number at a BS associated with a typical UE, can be expressed by deriving the probability density function (PDF) of the cell size [34]–[36]. In this study, N has to be derived by considering the building geometry since we consider non-homogeneous UE distributions.

To provide a more tractable mathematical representation, we assume UE number in the cell coverage of the BS associated with a typical UE to be its mean value as in [35], resulting in $E \left[\frac{1}{1+N} \right] \sim \frac{1}{1+E[N]}$. Although this assumption reduces the analytic accuracy, it does not significantly affect the tendency to rate \mathcal{R} as validated in Section V.

As mentioned in Section II, the UE density in the area near the buildings is different from that in the area far from the buildings. In the following lemma, the corresponding UE densities are given according to the user concentration ratio γ_c and the geography of buildings.

Lemma 2. The UE density λ is decomposed into the U_n density, λ_n , and the U_r density, λ_r , as follows.

$$\lambda_n = \lambda \gamma_c \left[1 + \frac{1 - 2\lambda_\ell(d_l + d_w)d_c - \lambda_\ell d_l d_w}{2\lambda_\ell(d_l + d_w)d_c} \right], \quad (8)$$

$$\lambda_r = \lambda(1 - \gamma_c) \left[1 + \frac{2\lambda_\ell(d_l + d_w)d_c}{1 - 2\lambda_\ell(d_l + d_w)d_c - \lambda_\ell d_l d_w} \right]. \quad (9)$$

Proof. A UE is U_n when the distance to its nearest building is less than d_c . Then a unit area can be divided into three parts: i) indoor area has an average size of $\lambda_\ell d_l d_w$, ii) U_n area, \mathcal{A}_n , has an average size of $\lambda_\ell 2(d_l + d_w)d_c$, and iii) U_r area, \mathcal{A}_r , occupies the rest. We assume that there is no overlapping area between buildings. so we can derive the densities λ_n and λ_r , respectively. ■

Note that the Lemma 2 enables us to calculate the mean UE number, leading to the following proposition.

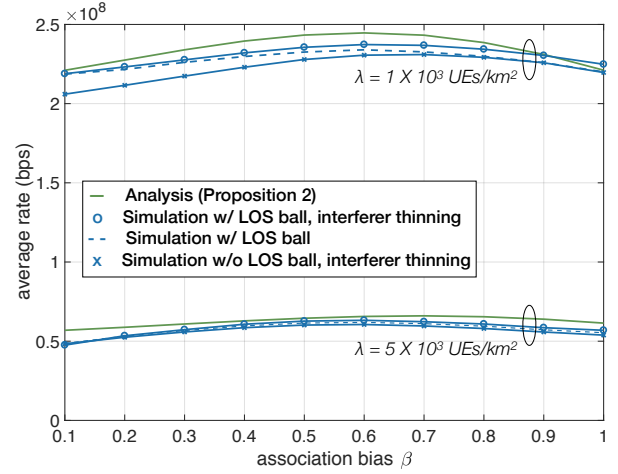


Fig. 6. Comparison of average rate with simulation results ($\lambda_b = 200$ BSs/km², $\lambda_\ell = 200$ buildings/km², $\theta = \frac{\pi}{6}$ rad, $d_l = 30$ m, $d_w = 10$ m, $t = 10$ dB, $\gamma_c = 0.6$, $g_m = 20$ dB, $g_s = 0$ dB).

Proposition 2. (Average Rate) The average rate using the building-aware association scheme is

$$\mathcal{R} = \frac{W\gamma_c}{1+N_n} \mathcal{S}_n(\beta) \log(1+t) + \frac{W(1-\gamma_c)}{1+N_r} \mathcal{S}_r(\beta) \log(1+t), \quad (10)$$

where N_n and N_r represent the mean number of UEs in the same cell coverage with a U_n and U_r , respectively, and are given as (12) and (11) at the bottom of the next page.

Proof. See Appendix. ■

In our algorithm, the O-BSs have to expand their cell coverages to fill the coverage hole resulting from the coverage reduction of D-BSs (see Fig. 4). In this regard, the event $R_\beta < 0.68\lambda^{-\frac{1}{2}}$ in (11) represents the case that a BS serving the typical UE has to expand the coverage since its neighboring BSs become D-BSs.

This analytic result is verified through simulation experiments rigorously carried out without approximations used in the analysis, e.g., average LOS region, uniform interfering BS thinning, and mean UE number. Fig. 6 compares the average rate from the analysis to that of PPP simulation. Although there is a slight gap between the two results due to the analytic assumptions, they follow a similar trend. Besides, when including the LOS ball model and homogeneous interferer thinning assumption discussed in Section III-A, the simulation result are more close to the analytic one. The reason the rate results from the simulations are generally lower than those from the analysis is two-fold. First, $E \left[\frac{1}{x} \right]$ is smaller than $\frac{1}{E[x]}$, which is utilized in the mean UE number approximation in Section III-B. Second, our analysis does not consider the case that the association distance of a typical UE might increase due to the building-aware association, as mentioned above. In addition, this figure shows that the difference between the optimal bias $\beta_{\mathcal{R}^*}$ from the analysis and the simulation is larger when the UE density is high. The reason behind is that the mean UE number approximation reduces the analytical accuracy when there are many UEs.

According to Proposition 2, mean UE numbers of the associated cell areas of U_n and U_r , i.e. N_n and N_r , have remarkable characteristics according to the bias β as follows.

Remark 2. *The average UE number N_r increases with the bias β while N_n decreases with it.*

The reason behind is that, when a typical UE is U_r , its associated BS is the farthest BS from the buildings in the LOS ball. Therefore as β increases, more neighboring BSs become D-BSs, increasing the typical cell coverage as well as the associated UE number. When a typical UE is U_n , probability that the associated BS becomes D-BS increases with β , resulting in the associated UE number decrement.

The remark also implies that the β increment decreases the amount of available bandwidth of a U_r , and vice versa for a U_n . Remember that higher β increases the SIR coverage of a U_r as explained in Remark 1. That is, β affects the available bandwidth and SIR coverage in opposite ways, leading us to derive the optimal β maximizing the average rate.

IV. RATE OPTIMAL BUILDING-AWARE ASSOCIATION

This section deals with the rate-maximizing bias β for the building-aware association algorithm. The optimal β derivation is not straightforward because our algorithm affects UE differently depending on whether the UE is close to a building or not. Furthermore, the bias β has the opposite effect on the SIR coverage and the amount of available bandwidth in the data rate of a typical UE.

Due to the additional UE number consideration, the optimal bias for maximizing the rate differs from that for maximizing the SIR coverage. In this section, we first focus on the optimal bias maximizing the SIR coverage, then provide the rate maximizing β .

As mentioned in Section III-A, the SIR coverage $\mathcal{S}_n(\beta)$ is maintained after $\beta = \tan\left(\frac{\theta}{2}\right)\frac{R_L}{d_l}$ that makes $R_\beta = \frac{R_L}{2}$, and $\mathcal{S}_r(\beta)$ increases with β . It implies that the SIR coverage \mathcal{S} is non-decreasing with β after $\beta = \tan\left(\frac{\theta}{2}\right)\frac{R_L}{d_l}$. This characteristic highly reduces the search range of β , leading to the following Proposition.

Proposition 3. (Optimal β) The optimal association bias is given as below.

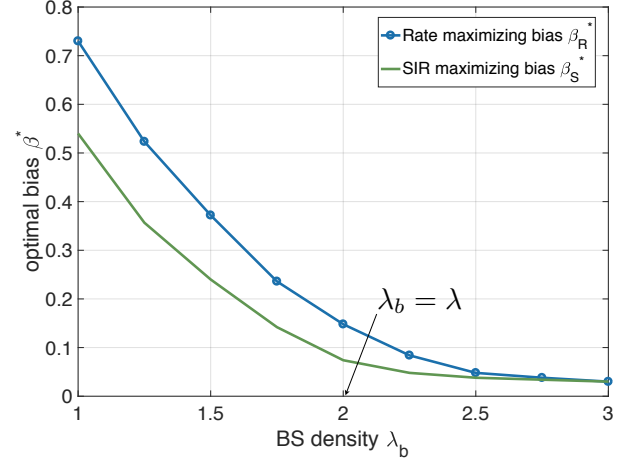


Fig. 7. SIR coverage and rate of the building-aware algorithm according to the association bias β ($\lambda_\ell = 300$ buildings/km², $\lambda = 2 \times 10^4$ UEs/km², $\theta = \frac{\pi}{4}$ rad, $d_l = 30$ m, $d_w = 10$ m, $t = 10$ dB, $\gamma_c = 0.6$, $g_m = 20$ dB, $g_s = 0$ dB).

- For maximizing the SIR coverage,

$$\beta_S^* = \begin{cases} \mathbb{1}_{C_1} + (1 - \mathbb{1}_{C_1}) \operatorname{argmax}_{T_\beta} \mathcal{S} & \text{if } R_L \tan\left(\frac{\theta}{2}\right) < d_l \\ \operatorname{argmax}_{0 \leq \beta \leq 1} \mathcal{S} & \text{otherwise} \end{cases} \quad (14)$$

$$\text{where } T_\beta = 0 \leq \beta \leq \tan\left(\frac{\theta}{2}\right)R_L d_l^{-1}, \\ C_1 := \gamma_c \mathcal{S}_n\left(\tan\left(\frac{\theta}{2}\right)\frac{R_L}{d_l}\right) + (1 - \gamma_c)\mathcal{S}_r(1) > \max_{T_\beta} \mathcal{S}.$$

- For maximizing the average rate,

$$\beta_{\mathcal{R}}^* = \operatorname{argmax}_{\beta} \frac{\gamma_c}{1 + N_n} \mathcal{S}_n(\beta) + \frac{(1 - \gamma_c)}{1 + N_r} \mathcal{S}_r(\beta). \quad (15)$$

Proof. See Appendix. ■

The result indicates that $\beta_S^* = 1$ if $\gamma_c = 0$ since $\mathcal{S}_r(\beta)$ monotonically increases with β . Also, it reveals that the optimal bias β_S^* decreases with the concentration ratio γ_c , because the SIR increment of a typical U_n is smaller than that of a typical U_r . Note that $\beta_{\mathcal{R}}^* \neq 1$ when $\gamma_c = 0$ due to the average UE number N_r increment along with β .

Although it is difficult to derive the optimal bias $\beta_{\mathcal{R}}^*$ in a closed form, it can be determined through a linear search using the above Proposition. Furthermore, we can obtain $\beta_{\mathcal{R}}^*$

$$N_r = \frac{1.28\lambda_r}{\pi\lambda_b R_\beta^2} \left(\mathbb{1}_{R_\beta < 0.68\sqrt{\lambda}} [(A_c - A_r)\lambda_n/\lambda_r + A_r] + \mathbb{1}_{R_\beta \geq 0.68\sqrt{\lambda}} \right) \quad (11)$$

$$N_n = \left(E(R_1, R_L)N_r + 0.64\beta d_l \left[\lambda_n c_1(d_c) + \left(d_c \lambda_n - \frac{d_c \lambda_r}{2} \right) E(d_c, R_1) + \lambda_r (c_1(R_1) - c_1(d_c)) \right] \right) / \left(1 - e^{-\frac{\pi\lambda_b R_L^2}{2}} \right) \quad (12)$$

$$\text{where } A_c = \max \left(\pi R_\beta^2, \pi R_L^2 - \frac{\beta d_l}{2} \left[\pi\lambda_b R_L (R_L^2 - R_\beta^2) - \frac{2}{3}\pi\lambda_b (R_L^3 - R_\beta^3) \right] \right) \quad \text{and} \quad (13)$$

$$A_r = \begin{cases} \pi (R_L - d_c)^2, & \text{if } d_c > R_L - R_\beta \\ \max \left(\pi R_\beta^2, \pi [R_L - d_c]^2 - \frac{\beta d_l \pi \lambda}{2} \left[(R_L - d_c) ([R_L - d_c]^2 - R_\beta^2) - \frac{2([R_L - d_c]^3 - [R_\beta - d_c]^3)}{3} \right] \right), & \text{otherwise.} \end{cases}$$

The function $E(a, b) = \exp(-\pi\lambda_b a^2/2) - \exp(\pi\lambda_b b^2/2)$, $c_1(x) = \operatorname{erf}\left(x\sqrt{\pi\lambda/2}\right)/\sqrt{2\lambda} - x \exp(-\pi\lambda_b x^2/2)$, and the indicator function $\mathbb{1}_{\mathbb{A}}$ returns 1 if the event \mathbb{A} occurs.

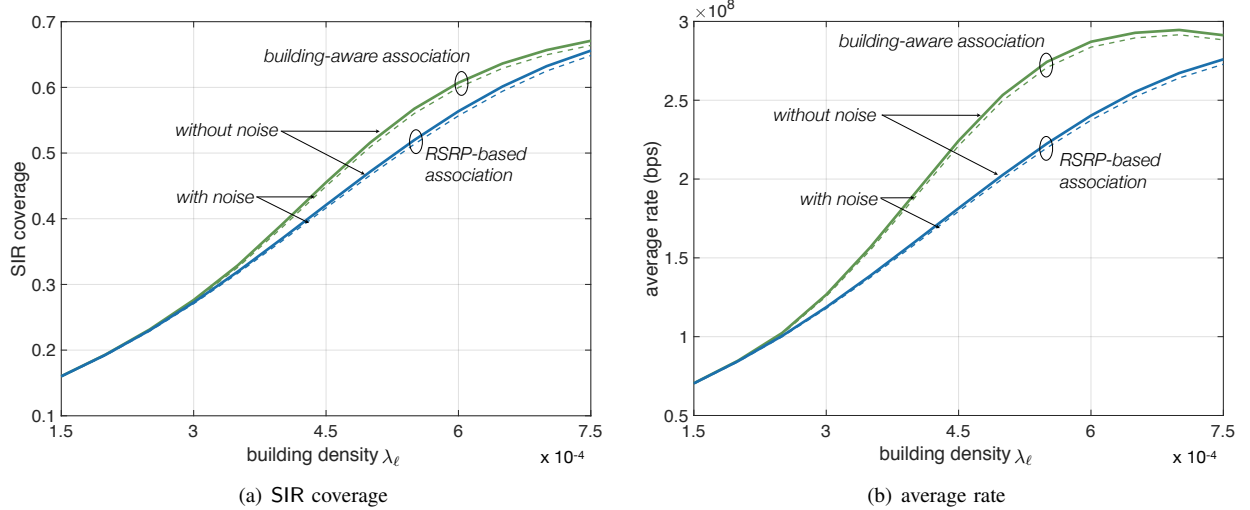


Fig. 8. Impact of building density λ_ℓ on SIR coverage and rate ($\lambda_b = 600$ BSs/km², $\lambda = 2 \times 10^3$ UEs/km², $\theta = \frac{\pi}{4}$, $\gamma_c = 0.6$).

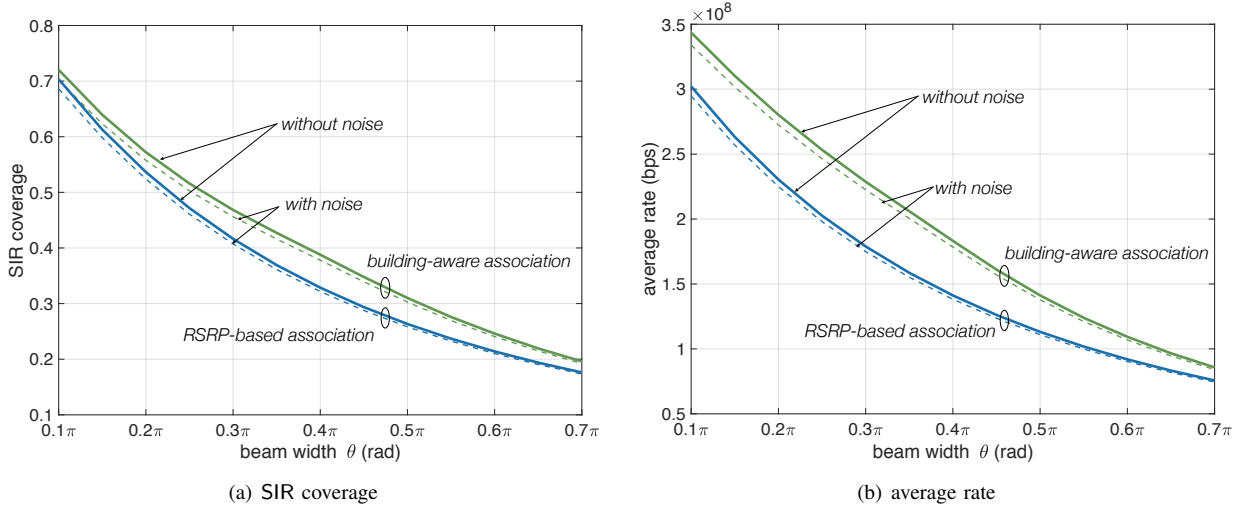


Fig. 9. Impact of beamwidth θ on SIR coverage and rate ($\lambda_b = 600$ BSs/km², $\lambda = 2 \times 10^3$ UEs/km², $\lambda_\ell = 500$ buildings/km², $\gamma_c = 0.6$).

more easily in the asymptotic case where the BS density is much higher than the UE density, as shown in the following Corollary.

Corollary 1. (Optimal Bias in Ultra-dense Scenario) When $\lambda_b \gg \lambda$, the mean UE number N_n and N_r converge to 0, i.e. $\lim_{\lambda/\lambda_b \rightarrow 0} N_n = 0$ and $\lim_{\lambda/\lambda_b \rightarrow 0} N_r = 0$. Thus, the optimal β for maximizing the SIR coverage and the rate become identical, i.e. $\beta_{\mathcal{R}}^* \sim \beta_{\mathcal{S}}^*$.

This Corollary provides the building-aware association design guideline for a special scenario that is asymptotic but highly in accordance with the BS densification trend, where the number of BSs exceed the UE number and some BSs may not serve any UE [5], [37]. By regarding $\beta_{\mathcal{R}}^* = \beta_{\mathcal{S}}^*$, we can efficiently diminish the calculation time due to the smaller searching range needed to find the optimal β . The accuracy of Corollary 1 is verified in Fig. 7.

In addition to this asymptotic case, the mathematical form in (15) provides a useful design guideline. This stems from the

intuition that there is an optimal ratio of D-BSs among the BSs in the LOS region to maximize the rate by jointly optimizing the SIR and the amount of available resources. Keeping this optimal ratio in mind, we summarize the building-aware association design guideline according to different network parameters, as in the following remarks.

Remark 3. The optimal bias $\beta_{\mathcal{R}}^*$ is affected by the network parameters as follows:

1. As the building density and/or length decreases, the optimal bias $\beta_{\mathcal{R}}^*$ should be increased.
2. As the beamwidth θ decreases, the optimal bias $\beta_{\mathcal{R}}^*$ should be decreased.

The reason behind is that as the building density and/or length decreases, the LOS region increases, resulting in an increment in the number of LOS BSs. Therefore, the optimal bias $\beta_{\mathcal{R}}^*$ should be increased to keep the optimal ratio of D-BSs among the BSs in the LOS region. On the otherhand, $\beta_{\mathcal{R}}^*$ increases with the beamwidth. This is because, when BSs

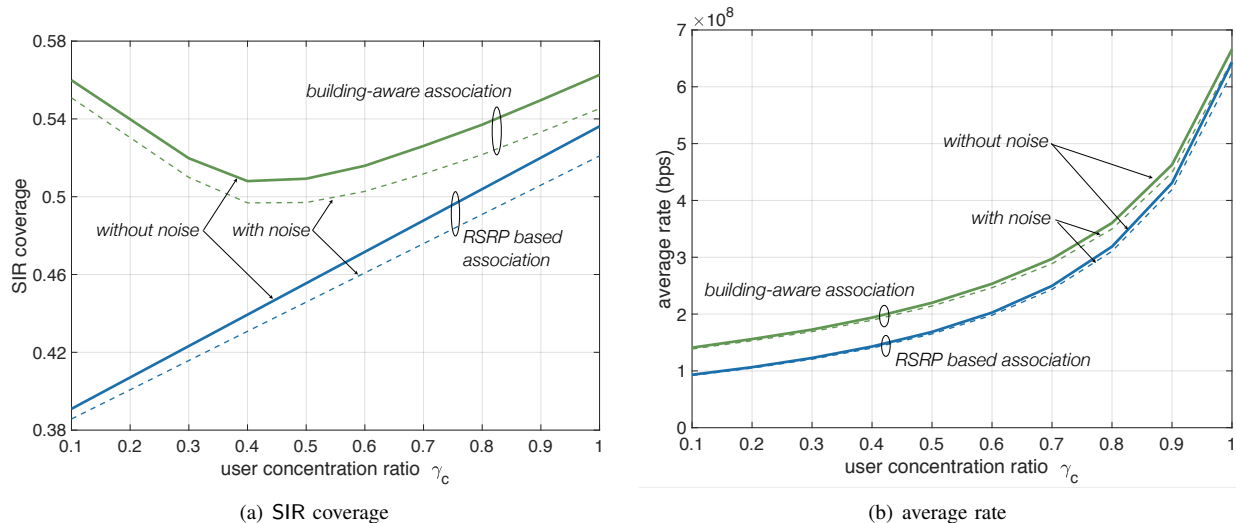


Fig. 10. Impact of user concentration ratio γ_c on SIR coverage and rate ($\lambda_b = 600$ BSs/km², $\lambda = 2 \times 10^3$ UEs/km², $\lambda_\ell = 500$ buildings/km², $\theta = \frac{\pi}{4}$).

TABLE I
BUILDING STATISTICS [5]

Building parameters (unit)	Manhattan	Gangnam	Chicago
Density (buildings/km ²)	1467	1010	474
Average length (m)	26.5	22.41	36.35
Average width (m)	20.83	9.35	21.48
Average LOS distance (m)	23.12	62.40	69.74

can transmit sharper beam signals, less BS beam signals leak beyond their nearest building, i.e. more BSs become D-BS by satisfying the D-BS condition (2) in Section II-D. Therefore, the optimal bias $\beta_{\mathcal{R}}^*$ should be decreased to keep the optimal ratio of D-BSs among BSs in the LOS region.

V. NUMERICAL EVALUATIONS OF BUILDING-AWARE ASSOCIATION ALGORITHM

The SIR coverage and rate of building-aware association scheme (Section III) and the corresponding optimal bias (Section IV) are evaluated in this section. In addition, the practical viability is validated by applying a real-world building geography in three cities, Gangnam, Manhattan, and Chicago.

A. SIR Coverage and Rate according to Different System Parameters

Figs. 8-10 visualize the SIR coverage and rate, according to the building density, beamwidth, and user concentration ratio, respectively. Default simulation parameters are given as follows: $W = 500$ MHz [17], $d_l = 30$ m, $d_i = 10$ m, $g_m = 20$ dB, $g_s = 0$ dB, $t = 10$ dB, transmit power = 23 dBm, and noise power = -77 dBm according to the following equation: -174 dBm/Hz + $10 \log_{10}(W \text{ Hz}) + 10$ dB. The association bias β by default is set to be the optimal value.

The three results show that the building-aware association scheme can achieve a superior SIR coverage and rate compared to the RSRP-based association scheme. In addition, they also illustrate the effect of considering noise power (see the dotted

lines). To this end, we additionally calculate the SINR coverage with minor modifications from the SIR coverage (7), by deviding the SINR coverage into SNR and SIR terms independently [38]. When considering the noise power, both the SIR coverage and rate decrease, but they still follow a similar trend as the results that do not consider the noise power, thus justifying the noise power elimination in our analysis.

Fig. 8 indicates that the gain of our algorithm does not monotonically increase with the building density λ_ℓ . This relates to the number of BSs that become D-BS using the algorithm. When λ_ℓ is small, there is not a sufficient number of BSs around the buildings, reducing the number of BSs that can become D-BS. The gain thus increases with λ_ℓ at first. However, when λ_ℓ is high, the number of BSs in the LOS region decreases due to the shrinkage of the LOS region. This also reduces the number of D-BS candidates, saturating the rate improvement. Fig. 9 shows that the building-aware association algorithm can complement the limitations of beam-forming technology. For instance, the building-aware association rate when $\theta = 0.3\pi$ is similar to that of the RSRP based association scheme when $\theta = 0.15\pi$, implying that the number of antennas can be reduced. Fig. 10 demonstrates that the SIR coverage gain using the building-aware association scheme decreases with the user concentration ratio γ_c whereas the rate gain does not. This is because the amount of SIR increment due to interference avoidance is high when most of the UEs are far from buildings (see Remark 1). On the other hand, the amount of rate increment by balancing the traffic load is high when most of UEs are adjacent to buildings so that the traffic unbalance is severe. Such load balancing gain compensates for the SIR gain decrement when γ_c is high.

B. Building-aware Association under a Real Building Geography

Using previous studies [5] and the open source geographic information, we calculate the building parameters for Gangnam, Manhattan, and Chicago as summarized in Table II.

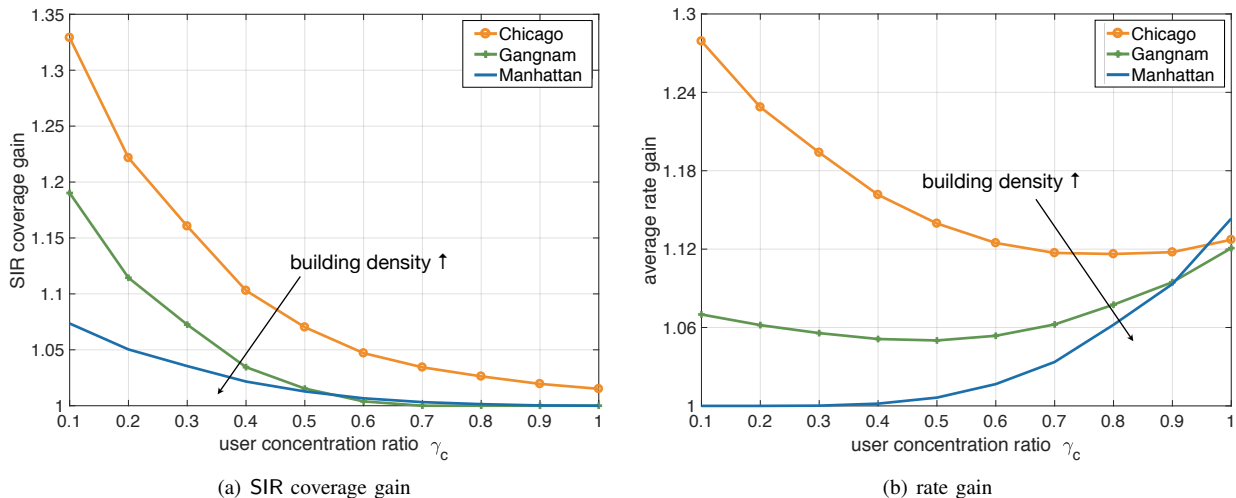


Fig. 11. SIR coverage and rate gain according to the user concentration ratio γ_c ($\lambda_b = 500$ BSs/km², $\lambda = 20 \times 10^3$ UEs/km², $\theta = \frac{\pi}{6}$ rad).

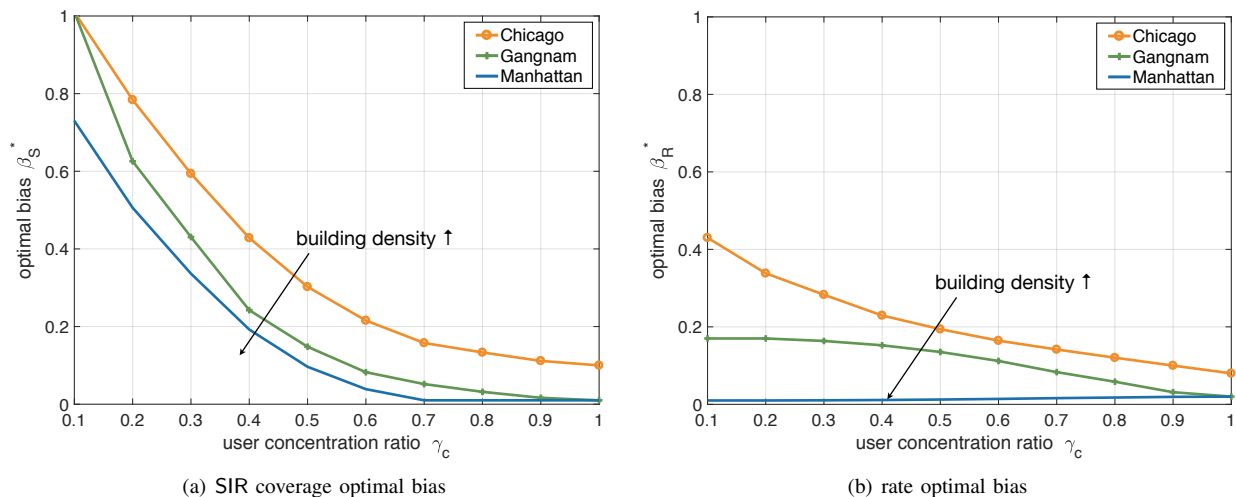


Fig. 12. Optimal biases for maximizing SIR coverage and rate according to the user concentration ratio γ_c ($\lambda_b = 500$ BSs/km², $\lambda = 20 \times 10^3$ UEs/km², $\theta = \frac{\pi}{6}$ rad).

Fig. 11 shows that the gain using the building-aware association scheme in Chicago is higher than that in Gangnam or Manhattan, implying that our algorithm is profitable in network geography like Chicago. The main reason behind is the building density λ_ℓ is smaller in Chicago compared to other cities. The corresponding large LOS region enables a sufficient number of BSs to become D-BS, leading to a further improvement in the average rate. As shown in Fig. 8 above, when λ_ℓ is too small or large the gain of proposed algorithm decreases. Besides, it is worth noting that the average building length in Chicago is longer than that in Gangnam and Manhattan. This implies that when the building length is long, there are more D-BS candidates around the buildings, increasing the feasible set of β to be optimized.

Although the rate gain in Manhattan is low compared to the gain in other cities, the average rate gain increases with the user concentration ratio γ_c . When UE is more frequently concentrated around buildings such as in dense urban scenarios

like Manhattan, the result implies that our algorithm can still guarantee a large improvement.

Fig. 12 illustrates that the optimal bias for the Manhattan scenario is low compared to that of the Gangnam and Chicago scenarios. This is mainly due to the fact that the LOS distance in Manhattan is short, thus there are a smaller number of BSs in the LOS region. Therefore, the optimal bias should be decreased to keep the optimal ratio of the number of D-BSs among BSs in the LOS region, as explained in Remark 3. This figure also shows that the optimal bias β_S^* is 1 when the ratio $\gamma_c = 0$ and then the optimal bias decreases.

VI. CONCLUSION

This study addresses the mmW interference problem due to the mmW BS densification and amplified directional signal strength. As a solution, we propose a building-aware association scheme where BSs adjacent to buildings only associate with UEs toward a building. The impact of this scheme is

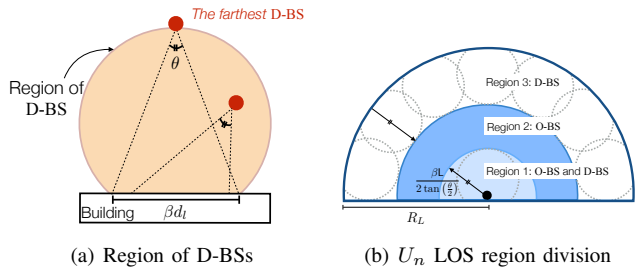


Fig. 13. Illustrations of D-BS condition (a) and region of D-BSs and O-BSs from the perspective of a typical U_n (b).

analyzed in terms of the average data rate using stochastic geometry (Proposition 2), verifying large improvements compared with the RSRP-based association scheme. The result indicates that the rate improvement is convex-shaped over the building density. In addition, it sheds light on obtaining the optimal association bias β that jointly optimizes the interference decrease and load balancing (Proposition 3). The result implies that the optimal bias β^* should be decreased with the building density and length, while it should be increased with the beamwidth. Real geography based blockage models in Gangnam, Manhattan and Chicago are used to validate the practical feasibility of the proposed algorithm, showing that our algorithm provides a higher rate improvement in Chicago scenario which has less buildings compared to other cities.

Further extension could contemplate the impact of UE mobility on traffic usage patterns. The traffic amount is known to have a convex-shape over the UE velocity [39]. Considering that UEs are likely to move at higher speeds when they are away from buildings (e.g., in-vehicle passengers), UEs far from buildings might cause more data traffic. By taking into account this behavior, we can provide an optimal association bias that better suits practical networks.

VII. APPENDIX

A. Proof of Lemma 1

In the average LOS ball model [18], a typical UE considers that there is a rectangular blockage at a distance R_L from it in all directions, implying that there are theoretically an infinite number of rectangular blockages at a distance R_L . Recall that a BS becomes a D-BS when its beam signal does not exceed the nearest building with length βd_l . Since the circumferential angles in the same arc of a circle are all equal, the region of D-BSs becomes a circle truncated by the building, where the circumferential angle is θ (see Fig. 13(a)). Then the distance from the building to its farthest D-BS becomes $\frac{\beta d_l}{2 \tan(\frac{\theta}{2})}$ using trigonometric properties. Since each blockage turns each BS within the maximum distance $\frac{\beta d_l}{2 \tan(\frac{\theta}{2})}$ from it to a D-BS and there are infinite blockages, the modified LOS area shrinks to have a radius of $R_\beta = \max\left(R_L - \frac{\beta d_l}{2 \tan(\frac{\theta}{2})}, 0\right)$.

B. Proof of Proposition 1

To derive the average SIR coverage, we calculate the SIR coverage of a typical U_r and that of a typical U_n respectively.

At first, $\mathcal{S}_r(\beta)$, the SIR coverage of U_r can be achieved through the following preliminary techniques.

- 1) **Distance Distribution under LOS Condition.** Define R as R_0 conditioned on $R_0 \leq R_L$. The cumulative density function (CDF) of R is

$$\begin{aligned} \mathbb{P}(R > r) &:= \mathbb{P}(R_0 > r | R_0 \leq R_L) = \frac{\mathbb{P}(r < R_0 \leq R_L)}{\mathbb{P}(R_0 \leq R_L)} \\ &= \frac{\mathbb{P}(R_0 > r) - \mathbb{P}(R_0 > R_L)}{\mathbb{P}(R_0 \leq R_L)}. \end{aligned} \quad (16)$$

By differentiating (16), we can get the PDF of R : $f_R(r) = \frac{f_{R_0}(r)}{\mathbb{P}(R_0 \leq R_L)}$, where $f_{R_0}(r) = 2\pi\lambda_b r \exp(-\pi\lambda_b r^2)$.

- 2) **Directional Interference Thinning.** Now that BSs transmit directional signal, the interfering BSs are decomposed into two groups: who transmit interfering signals with the antenna gain g_m and g_s . Since the probability that angle from a BS is within the beamwidth θ is $\frac{\theta}{2\pi}$, each BS's link to a typical user has a gain g_m with probability $\frac{\theta}{2\pi}$ and g_s with probability $1 - \frac{\theta}{2\pi}$. According to the mapping theorem, the power decrease with $\frac{g_s}{g_m}$ has an equal effect with density decrease with $\left(\frac{g_s}{g_m}\right)^{\frac{2}{\alpha}}$ [5]. The actual interferer thus can be thinned with a probability $p_a = \frac{\theta}{2\pi} + \frac{2\pi - \theta}{2\pi} \left(\frac{g_s}{g_m}\right)^{\frac{2}{\alpha}}$.

The SIR coverage then is represented as below.

$$\begin{aligned} \mathcal{S}_r(\beta) &= \mathbb{P}(R_0 \leq R_L) \int_0^{R_L} \mathbb{P}\left(\frac{g_m r^{-\alpha} h}{\sum_{x_i \in \Phi_b(\lambda_b)} G_i |x_i|^{-\alpha} h_i} > t\right) f_{R_0}(r) dr \end{aligned} \quad (17)$$

$$\begin{aligned} &\stackrel{(a)}{=} \int_0^{R_\beta} \mathbb{P}\left(\frac{g_m r^{-\alpha} h}{\sum_{x_i \in \Phi_b(\lambda_b)} G_i |x_i|^{-\alpha} h_i} > t\right) f_{R_0}(r) dr \\ &+ \int_{R_\beta}^{R_L} \mathbb{P}\left(\frac{r^{-\alpha} h}{\sum_{x_i \in \Phi_b(\lambda_b)} \frac{g_s}{g_m} |x_i|^{-\alpha} h_i} > t\right) f_{R_0}(r) dr \end{aligned} \quad (18)$$

$$\begin{aligned} &\stackrel{(b)}{=} \int_0^{R_\beta} \exp\left(-\pi\lambda_b r^2 \left[p_a t^{\frac{2}{\alpha}} \int_{t^{-\frac{2}{\alpha}}}^{\frac{R_\beta^2}{r^2 t^{\frac{2}{\alpha}}}} \frac{du}{1+u^{\frac{\alpha}{2}}} \right. \right. \\ &\left. \left. + \left(\frac{g_s t}{g_m}\right)^{\frac{2}{\alpha}} \int_{\frac{R_\beta^2}{r^2 t^{\frac{2}{\alpha}}}}^{\frac{R_L^2}{r^2 t^{\frac{2}{\alpha}}}} \frac{du}{1+u^{\frac{\alpha}{2}}} \right]\right) f_{R_0}(r) dr \\ &+ \int_{R_\beta}^{R_L} \exp\left(-\pi\lambda_b r^2 \left[\left(\frac{g_s t}{g_m}\right)^{\frac{2}{\alpha}} \int_{t^{-\frac{2}{\alpha}}}^{\frac{R_L^2}{r^2 t^{\frac{2}{\alpha}}}} \frac{du}{1+u^{\frac{\alpha}{2}}} \right]\right) f_{R_0}(r) dr, \end{aligned} \quad (19)$$

where $R_1 = \min\left(R_L - R_\beta, \frac{R_L}{2}\right)$, $r_1 = \max\left[\max\left(R_\beta, \frac{R_L}{2}\right)^2, r^2\right] \left(rt^{\frac{1}{\alpha}}\right)^{-2}$, $r_2 = \min\left(R_L - R_\beta, \frac{R_L}{2}\right)^2 \left(rt^{\frac{1}{\alpha}}\right)^{-2}$. Step (a) follows from that when the signal distance is longer than R_β , a typical U_r receives interference signal only with a side lobe gain g_s . In addition, step (b) follows from: (i) directional interference thinning with mapping theorem and (ii) the modified LOS region. By applying $f_{R_0}(r)$ and integrating it from R_β to R_L , we can derive the $\mathcal{S}_r(\beta)$.

The SIR coverage of a typical U_n differs from that of a typical U_r because their LOS regions are different and some D-BSs can interfere a U_n .

- 1) **Distance Distribution.** Remind that a typical U_n has a half moon shaped LOS region due to the building on its side. This implies that a U_n cannot receive signals from BSs on the other side of the building, making the signal distance PDF different as below.

$$f_{R_0}(r) = \pi \lambda_b r \exp\left(-\frac{\pi \lambda_b r^2}{2}\right). \quad (20)$$

- 2) **Interference Division.** In order to calculate the interference of a typical U_n , we separate the LOS region into three regions as shown in Fig. 13(b). Firstly, in region 1, there are D-BSs and O-BSs. Since D-BSs in this region transmit signals toward the building where the U_n is attached, we assume that their signals always interfere with U_n . Secondly, in region 2, there are only O-BSs. They interfere with U_n if their signal directions are toward the U_n . Thirdly, in region 3, there are only D-BSs who transmit signals toward UEs on their nearest buildings side, causing side lobe interference to the U_n .

- 3) **Probability of Being Interferer in Region 1.** Since the probability of a BS in region 1 interfering with the U_n depends on whether it is a D-BS or a O-BS, it is important to derive the probability of a BS being D-BS. The probability is derived by the ratio of the area of region 1 to the truncated circle inside region 1 as follows: $\left(\frac{(\pi-\theta)^2}{4\sin^2(\theta)} + \frac{1}{4\tan(\theta)}\right) \frac{8\tan^2(\frac{\theta}{2})}{\pi}$. By considering this probability and main lobe interfering probability, the probability P_ℓ that a BS in region 1 becomes a main lobe interferer is $P_\ell = \left(\frac{(\pi-\theta)^2}{4\sin^2(\theta)} + \frac{1}{4\tan(\theta)}\right) \frac{8\tan^2(\frac{\theta}{2})}{\pi} + \left[1 - \left(\frac{(\pi-\theta)^2}{4\sin^2(\theta)} + \frac{1}{4\tan(\theta)}\right) \frac{8\tan^2(\frac{\theta}{2})}{\pi}\right] p_a$.

By utilizing the distance distribution and interference division, we can derive the SIR coverage of a typical U_n as follows.

$$\begin{aligned} \mathcal{S}_n(\beta) &= \mathbb{P}(R_0 \leq R_L) \int_0^{R_L} \mathbb{P}\left(\frac{g_m r^{-\alpha} h}{\sum_{x_i \in \Phi_b(\lambda_b)} G_i |x_i|^{-\alpha} h_i} > t\right) f_{R_0}(r) dr \\ &= \int_{\max(R_\beta, \frac{R_L}{2})}^{R_L} \mathbb{P}\left(\frac{r^{-\alpha} h}{\sum_{x_i \in \Phi_b(\lambda_b)} \frac{g_s}{g_m} |x_i|^{-\alpha} h_i} > t\right) f_{R_0}(r) dr \\ &+ \int_0^{\max(R_\beta, \frac{R_L}{2})} \mathbb{P}\left(\frac{g_m r^{-\alpha} h}{\sum_{x_i \in \Phi_b(\lambda_b)} G_i |x_i|^{-\alpha} h_i} > t\right) f_{R_0}(r) dr \\ &\stackrel{(a)}{=} \int_{R_1}^{R_L} \pi \lambda_b r \exp\left[-\frac{\pi \lambda_b r^2}{2} \left(1 + p_a t^{\frac{2}{\alpha}} \int_{t^{-\frac{2}{\alpha}}}^{r_1} \frac{du}{1+u^{\frac{\alpha}{2}}}\right.\right. \\ &\quad \left.\left.+ \left[\frac{g_s t}{g_m}\right]^{\frac{2}{\alpha}} \int_{r_1}^{\frac{R_L}{2}} \frac{du}{1+u^{\frac{\alpha}{2}}}\right)\right] dr \\ &+ \int_0^{R_1} \pi \lambda_b r \exp\left[-\frac{\pi \lambda_b r^2}{2} \left(1 + P_\ell t^{\frac{2}{\alpha}} \int_{t^{-\frac{2}{\alpha}}}^{r_2} \frac{du}{1+u^{\frac{\alpha}{2}}}\right.\right. \\ &\quad \left.\left.+ p_a t^{\frac{2}{\alpha}} \int_{r_2}^{r_1} \frac{du}{1+u^{\frac{\alpha}{2}}} + \left[\frac{g_s t}{g_m}\right]^{\frac{2}{\alpha}} \int_{r_1}^{\frac{R_L}{2}} \frac{du}{1+u^{\frac{\alpha}{2}}}\right)\right] dr, \quad (23) \end{aligned}$$

where (a) follows from the division of interference region. When the association distance r is shorter than $\min(R_L - R_\beta, \frac{R_L}{2})$, D-BS's in region 1 and O-BSs in region 1 and 2 can interfere with the U_n but their corresponding probabilities of being interferer are different.

Note that the path-loss exponent α in mmW networks is small compared to that used in the conventional sub-6 GHz frequency since we only consider LOS communication links [30]. Considering that α cannot be smaller than 2 when we observe a 2-dimensional space [24], we only focus on the case that α larger than 2 goes to it, i.e. $\alpha \rightarrow 2+$. For the exponent α close to 2, we can remove double integration in (19) and (23) by using a property $\lim_{\alpha \rightarrow 2} \int \frac{dx}{1+x^{\frac{\alpha}{2}}} = \ln(1+x)$. Then the SIR coverage $\mathcal{S}_r(\beta)$ (19) is simplified as below.

$$\begin{aligned} \lim_{\alpha \rightarrow 2+} \mathcal{S}_r(\beta) &= 2F_0^{R_\beta} \left(2 + 2p_a t \int_{t^{-1}}^{\frac{R_\beta}{r^{2t}}} \frac{du}{1+u} + \frac{2g_s t}{g_m} \int_{\frac{R_L}{r^{2t}}}^{\frac{R_L}{r^{2t}}} \frac{du}{1+u}\right) \\ &+ 2F_{R_\beta}^{R_L} \left(2 + \frac{2g_s t}{g_m} \int_{t^{-1}}^{\frac{R_L}{r^{2t}}} \frac{du}{1+u}\right) \\ &= 2F_0^{R_\beta} \left[2 + 2p_a t \ln\left(\frac{t+R_\beta^2 r^{-2}}{1+t}\right) + \frac{2g_s t}{g_m} \ln\left(\frac{t+R_L^2 r^{-2}}{t+R_\beta^2 r^{-2}}\right)\right] \\ &+ 2F_{R_\beta}^{R_L} \left[2 + \frac{2g_s t}{g_m} \ln\left(\frac{t+R_L^2 r^{-2}}{t+1}\right)\right] \quad (25) \end{aligned}$$

The same process is applied to derive $\mathcal{S}_n(\beta)$.

By applying $\mathcal{S}_r(\beta)$ and $\mathcal{S}_n(\beta)$ into $\mathbb{P}(\text{SIR} > t) = (1 - \gamma_c) \mathcal{S}_r(\beta) + \gamma_c \mathcal{S}_n(\beta)$, we can finalize the proof. ■

C. Proof of Proposition 2

We need to calculate the average UE number in the cell coverage for a typical UE N_n and N_r .

1) *Derivation of N_r :* When $\beta = 0$, i.e. there are no D-BS, $N_r = \frac{1.28\lambda_r}{\lambda}$ since a typical cell is 1.28 times larger than other cells on average [35] and the typical cell is located near the center of the LOS ball and assumed to have no U_n 's who are attached to buildings. As β increases, O-BSs should expand their association areas when their neighboring BSs become D-BS and shrink their coverage areas. To check if any neighboring BSs of a typical cell become D-BS, we consider that the average number of neighboring BSs of a typical BS in two-dimensions is 6 [33] and the average distance to the 6-th nearest neighboring node from a typical U_r is $\frac{0.68}{\sqrt{\lambda}}$ [24]. For computational brevity, we assume that the typical cell expands its cell area when $\frac{0.68}{\sqrt{\lambda}} > R_\beta$, i.e. when its 6-th nearest neighboring BS becomes D-BS. Otherwise, it keeps its association area.

To derive the average expanded area of the typical cell, we need to calculate the area of an O-BS. The area of an O-BS is derived by assuming that the association region of a D-BS is equal to a triangle whose base line length is βd_i and height

is the distance to the building.

$$\begin{aligned} E & \left(\pi R_L^2 - \sum_{R_\beta \leq r_i \leq R_L} \frac{\beta d_l}{2} (R_L - r_i) \right) \\ & = \pi R_L^2 - \frac{\beta d_l}{2} \int_{R_\beta}^{R_L} 2\pi \lambda_b r (R_L - r) dr \\ & = \pi R_L^2 - \frac{\beta d_l}{2} \left[\pi \lambda_b R_L (R_L^2 - R_\beta^2) - \frac{2\pi \lambda_b (R_L^3 - R_\beta^3)}{3} \right]. \end{aligned} \quad (26)$$

Since we do not consider the overlapping region among D-BS association regions, the above area may be smaller than πR_β^2 . Thus we derive the average area of O-BS as below.

$$A_c = \max \left(\pi R_\beta^2, \pi R_L^2 - \frac{\beta d_l}{2} [\pi \lambda_b R_L (R_L^2 - R_\beta^2) - \frac{2}{3} \pi \lambda_b (R_L^3 - R_\beta^3)] \right). \quad (28)$$

Since the association area of an O-BS is expanded from πR_β^2 to A_c , the average association area of the typical cell becomes $\frac{1.28 A_c}{\lambda_b \pi R_\beta^2}$. Within the area of an O-BS, there are U_r 's and U_n 's. To derive the average UE number in the typical cell coverage, we calculate the area of U_r 's A_r . If $d_c > R_L - R_\beta$, the area A_r becomes $\pi (R_L - d_c)^2$. Otherwise, by calculating $E \left[\sum_{R_\beta \leq r_i \leq R_L - d_c} \frac{\beta d_l}{2} (R_L - r_i - d_c) \right]$, the area A_r becomes

$$A_r = \max \left(\pi R_\beta^2, \pi [R_L - d_c]^2 - \frac{\beta d_l \pi \lambda}{2} [(R_L - d_c) ((R_L - d_c)^2 - R_\beta^2) - \frac{2}{3} ((R_L - d_c)^3 - [R_\beta - d_c]^3)] \right). \quad (29)$$

Then the average UE number in the typical cell N_r becomes $\frac{1.28[(A_c - A_r)\lambda_n + A_r\lambda_r]}{\lambda_b \pi R_\beta^2}$.

2) *Derivation of N_n* : The area of a typical cell depends on the association distance r . When $0 \leq r < d_c$, there are only U_n 's in the association area of the typical cell. Since the associated BS is D-BS and its average cell area is $\frac{1.28\beta d_l r}{2}$, the average UE number in the typical cell becomes $\frac{1.28\beta d_l r \lambda_n}{2}$. When $d_c \leq r < \min(R_L - R_\beta, \frac{R_L}{2})$, the associated BS is still a D-BS and its average cell area is $\frac{1.28\beta d_l r}{2}$ but there are both of U_n 's and U_r 's. So the average UE numbers becomes $1.28\beta d_l (\frac{r-d_c}{2} \lambda_r + d_c \lambda_n)$. When $\min(R_L - R_\beta, \frac{R_L}{2}) \leq r \leq R_L$, the BS could be a D-BS or not, and the average UE number thus is similar to N_r . By applying the signal distance distribution of N_n (20), we can finalize the proof. ■

D. Proof of Proposition 3

If $\beta > \frac{R_L \tan(\frac{\theta}{2})}{d_l}$, the coverage $\mathcal{S}_n(\beta)$ no longer depends on β . Also we know that the coverage $\mathcal{S}_r(\beta)$ is monotonically increasing with β . The optimal β in the interval from $\frac{R_L \tan(\frac{\theta}{2})}{d_l}$ to 1 thus become 1. What we have to do is then to compare $\gamma_c \mathcal{S}_n \left(\frac{R_L \tan(\frac{\theta}{2})}{d_l} \right) + (1 - \gamma_c) \mathcal{S}_r(1)$ and $\max_{0 \leq \beta \leq R_L \tan(\frac{\theta}{2})/d_l} \gamma_c \mathcal{S}_n(\beta) + (1 - \gamma_c) \mathcal{S}_r(\beta)$, which is the maximum SIR coverage in the interval $0 \leq \beta \leq \frac{R_L \tan(\frac{\theta}{2})}{d_l}$. ■

REFERENCES

- [1] T. S. Rappaport *et al.*, "Millimeter wave mobile communications for 5G cellular: it will work!," *IEEE Access*, vol. 1, pp. 335–349, May 2013.
- [2] S. Ragan, T. S. Rappaport, and E. Erkip, "Millimeter-wave cellular wireless networks: potentials and challenges," *Proceedings of the IEEE*, vol. 102, no. 3, pp. 366–385, Mar. 2014.
- [3] Ericsson, "5G radio access," *Ericsson Review*, Feb. 2015.
- [4] Y. Niu, Y. Li, D. Jin, L. Su, A. V. Vasilakos, "A survey of millimeter wave communications (mmWave) for 5G: opportunities and challenges," *Wireless Netw.*, vol. 21, no. 8 pp. 2657–2676, Apr. 2015.
- [5] J. Park, S.-L. Kim, and J. Zander, "Tractable resource management with uplink decoupled millimeter-wave overlay in ultra-dense cellular networks," *IEEE trans. wireless commun.*, vol. 15, no. 6, pp. 4362–4379, Jun. 2016.
- [6] E. Hossain, D. I. Kim, and V. K. Bhargava, *Cooperative cellular wireless networks*, Cambridge University Press, 2011.
- [7] C. Yang, S. Han, X. Hou, and A. F. Molisch, "How do we design CoMP to achieve its promised potential?," *IEEE Wireless Commun.*, vol. 20, no. 1, pp. 67–74, Feb. 2013.
- [8] J. Gehl, "Life between buildings: using public space," *Island Press*, 2011.
- [9] B. Hofmann-Wellenhof, K. Legat, and M. Wieser, "Navigation: principles of positioning and guidance," *Springer-Verlag Wien*, 2003.
- [10] R. T. LeGates and F. Stout, Ed. "The city reader," *Routledge*, 2015.
- [11] 3GPP TR 36.912 V14.0.0, "3GPP; Technical Specification Group Radio Access Network; Feasibility study for Further Advancements for E-UTRA (LTE-Advanced) (Release 14)," Mar. 2017.
- [12] J. Bae, Y. S. Choi, J. S. Kim, M. Y. Chung, "Architecture and performance evaluation of MmWave based 5G mobile communication system," in *Proc. IEEE International Conference on Information and Communication Technology Convergence (ICTC)*, Busan, Korea, Oct. 2014, pp. 847–851.
- [13] Z. Marzi, U. Madhow, H. Zheng, "Interference analysis for mm-wave picocells," in *Proc. IEEE Global Communications Conference (GLOBECOM)*, San Diego, CA, United States, Dec. 2015, pp. 1–6.
- [14] F. Boccardi, H. Shokri-Ghadikolaei, G. Fodor, E. Erkip, C. Fischione, M. Kountouris, P. Popovski, and M. Zorzi, "Spectrum pooling in mmwave networks: Opportunities, challenges, and enablers," *IEEE Commun. Mag.*, vol. 54, no. 11 pp. 33–39, Nov. 2016.
- [15] X. An, C.-S. Sum, R. V. Prasad, J. Wang, Z. Lan, J. Wang, R. Hekmat, H. Harada, and I. Niemegeers, "Beam switching support to resolve link-blockage problem in 60 GHz WPANs," in *Proc. IEEE International Symposium on Personal, Indoor and Mobile Radio Communications (PIMRC)*, Tokyo, Japan, Sep. 2009, pp. 390–394.
- [16] S. Singh, F. Ziliotto, U. Madhow, E. M. Belding, and M. Rodwell, "Blockage and directivity in 60 GHz wireless personal area networks: from cross-layer model to multihop MAC design," *IEEE J. Sel. Areas. Commun.*, vol. 27, no. 8, pp. 1400–1413, Oct. 2009.
- [17] Nokia, "The 5G mmWave revolution," *Nokia White Paper*, Sep. 2016.
- [18] T. Bai, R. Vaze, and R. W. Heath, Jr., "Analysis of blockage effects on urban cellular networks," *IEEE Trans. Wireless Commun.*, vol. 13, no. 9, pp. 5070–5083, Sep. 2014.
- [19] J. G. Andrews, T. Bai, M. N. Kulkarni, A. Alkhatieb, A. K. Gupta, and R. W. Heath, Jr., "Modeling and analyzing millimeter wave cellular systems," *IEEE Trans. Commun.*, vol. 65, no. 1, pp. 403–430, Jan. 2017.
- [20] M. R. Akdeniz, Y. Liu, M. K. Samimi, S. Sum, S. Rangan, T. S. Rappaport, and E. Erkip, "Millimeter wave channel modeling and cellular capacity evaluation," *IEEE J. Sel. Areas. Commun.*, vol. 32, no. 6, pp. 1164–1179, Jun. 2014.
- [21] T. Bai, and R. W. Heath, Jr., "Coverage and rate analysis for millimeter-wave cellular networks," *IEEE Trans. Wireless Commun.*, vol. 14, no. 2, pp. 1100–1114, Feb. 2015.
- [22] A. Baddeley and R. Turner, *Modeling spatial point patterns in R*, New York:Springer, pp.3–48, 2006.
- [23] D. Karlis and E. Xekalaki, "Mixed poisson distributions," *Int. Statist. Rev.*, vol. 73, no. 1, pp. 35–58, 2005.
- [24] D. Stoyan, W. S. Kendall, and J. Mecke, *Stochastic geometry and its applications*, Wiley, 2nd edition, 1995.
- [25] X. Yu, J. Zhang, M. Haenggi, and K. B. Letaief, "Coverage analysis for millimeter wave networks: the impact of directional antenna arrays," Apr. 2017, available at: <https://arxiv.org/pdf/1702.04493.pdf>.
- [26] H. Elshaer, M. N. Kulkarni, F. Boccardi, J. G. Andrews, and M. Dohler, "Downlink and uplink cell association with traditional macrocells and millimeter wave small cells," *IEEE Trans. Wireless Commun.*, vol. 15, no. 9, pp. 6244–6258, Sep. 2016.

- [27] Y. Li, J. G. Andrews, F. Baccelli, T. D. Novlan, and C. Zhang, "Design and analysis of initial access in millimeter wave cellular networks," available at: <https://arxiv.org/abs/1609.05582>.
- [28] A. K. Gupta, J. G. Andrews, and R. W. Heath, "On the feasibility of sharing spectrum licenses in mmwave cellular systems," *IEEE Trans. Commun.*, vol. 64, pp. 3981–3995, Sept. 2016.
- [29] D. N. C. Tse and P. Viswanath *Fundamentals of wireless communications*, Cambridge University Press, 2005.
- [30] A. I. Sulyman, A. T. Nassar, M. K. Samimi, G. R. MacCartney Jr., T. S. Rappaport, and A. Alsanie, "Radio propagation path loss models for 5G cellular networks in the 28 GHz and 38 GHz millimeter-wave bands," *IEEE Commun. Mag.*, vol. 52, no. 9, pp. 78–86, Sep. 2014.
- [31] M. Giordani, M. Mezzavilla, and M. Zorzi, "Initial access in 5G mm-Wave cellular networks," *IEEE Commun. Mag.*, vol. 54, no. 11, pp. 40–47, Nov. 2016.
- [32] 3GPP TS 36.331, V14.4.0, "3GPP; Technical Specification Group Radio Access Network; E-UTRA Radio Resource Control (RRC); Protocol Specification (Release 14)," Sep. 2017.
- [33] M. Tanemura, "Statistical distributions of poisson Voronoi cells in two and three dimensions," *FORMA-TOKYO* vol. 18, no. 4, pp. 221–247, 2003.
- [34] S. M. Yu, and S-L Kim, "Downlink capacity and base station density in cellular networks," in *Proc. IEEE WiOpt Workshop Spatial Stochastic Models Wireless Netw. (SpaWiN13)*, Tsukuba Science City, Japan, May 2013, pp. 119–124.
- [35] S. Singh, H. S. Dhillon, and J. G. Andrews, "Offloading in heterogeneous networks: Modeling, analysis, and design insights," *IEEE Trans. Wireless Commun.*, vol. 12, no. 5, pp. 2484–2497, May 2013.
- [36] J. Kim, J. Park, S.-W. Ko, and S.-L. Kim, "User attraction via wireless charging in cellular networks," in *Proc. IEEE WiOpt Workshop on Green Networks (GREENNET'16)*, Tempe, Arizona, United States, May 2016, pp. 91–98.
- [37] J. Park, S.-L. Kim, and J. Zander, "Asymptotic behavior of ultra-dense cellular networks and its economic impact," in *Proc. IEEE Global Communications Conference (GLOBECOM)*, Austin, TX, United States, Dec. 2014, pp. 4941–4946.
- [38] J. G. Andrews, F. Baccelli, and R. K. Ganti, "A tractable approach to coverage and rate in cellular networks," *IEEE Trans. Wireless Commun.*, vol. 59, no. 11, pp. 3122–3134, Nov. 2011.
- [39] T. Shim, J. Park, S.-W. Ko, S.-L. Kim, B. Lee, and J. Choi, "Traffic convexity aware cellular networks: a vehicular heavy user perspective," *IEEE Wireless Commun.*, vol. 23, no.1, pp. 88–94, Feb. 2016.



Jeemin Kim received the B.S. degree in electronic engineering from Ewha Womans University, Seoul, Korea, in 2012. She is currently working toward the combined Master's and Doctoral degrees in electrical and electronic engineering from Yonsei University, Seoul, Korea.

She was a Visiting Doctoral Student with Wireless@KTH, Royal Institute of Technology, Kista, Sweden. Her research interests include IoT communications, dynamic spectrum access, millimeter-wave communications, resource management, and

stochastic geometric approach to analysis network interference.



Jihong Park received his B.S. and Ph.D. degrees in electrical and electronic engineering from Yonsei University, Seoul, Korea, respectively in 2009 and 2016. He is currently a Postdoctoral researcher at Aalborg University, Denmark. He received the 2014 IEEE GLOBECOM travel grant, the 2014 IEEE Seoul Section Student Paper Contest Bronze Prize, and the 6th IDIS-ETNEWS (The Electronic Times) Paper Contest Award sponsored by the Ministry of Science, ICT, and Future Planning of Korea.

He was a visiting researcher at the Department of Applied Mathematics, Hong Kong Polytechnic University, at the Department of Communication Systems, the KTH Royal Institute of Technology, Stockholm, Sweden, at the Department of Electronic Systems, Aalborg University, Denmark, and at the Department of Electrical and Computer Engineering, New Jersey Institute of Technology, USA, respectively in 2013, 2015, 2016, and 2017. His research interests include ultra-dense/ultra-reliable/massive-MIMO wireless system designs using stochastic geometry, network economics, and communication theory.

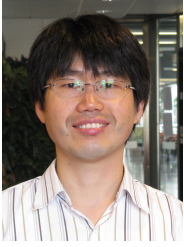


Seunghwan Kim received his B.S. degree in electrical and electronic engineering from Yonsei University, Seoul, Korea, in 2015. He is currently pursuing a combined Master's and Doctoral program in the School of Electrical and Electronic Engineering at the same university. His current research includes radio resource management, interference-limited networks, dual connectivity, power control, and network simulator implementation.



Seong-Lyun Kim is a Professor of wireless networks at the School of Electrical & Electronic Engineering, Yonsei University, Seoul, Korea, heading the Radio Resource Management & Optimization (RAMO) Laboratory and the Center for Flexible Radio (CFR+). He was an Assistant Professor of Radio Communication Systems at the Department of Signals, Sensors & Systems, Royal Institute of Technology (KTH), Stockholm, Sweden. He was a Visiting Professor at the Control Group, Helsinki University of Technology (now Aalto), Finland, and

the KTH Center for Wireless Systems. He served as a technical committee member or a chair for various conferences, and an editorial board member of *IEEE Transactions on Vehicular Technology*, *IEEE Communications Letters*, *Elsevier Control Engineering Practice*, and *Journal of Communications and Network*. He served as the leading guest editor of *IEEE Wireless Communications*, and *IEEE Network* for wireless communications in networked robotics. His research interest includes radio resource management and information theory in wireless networks, economics of wireless systems, and robotic networks. He published numerous papers, including the co-authored book (with Prof. Jens Zander), *Radio Resource Management for Wireless Networks* (Artech House, Inc.).



Ki Won Sung (M'10) is a Docent researcher in the Communication Systems Department at KTH Royal Institute of Technology, Stockholm, Sweden. He is also affiliated with KTH Center for Wireless Systems (Wireless@kth). He received a B.S. degree in industrial management, and M.S. and Ph.D. degrees in industrial engineering from Korea Advanced Institute of Science and Technology (KAIST) in 1998, 2000, and 2005, respectively. From 2005 to 2007 he was a senior engineer in Samsung Electronics, Korea, where he participated in the development and commercialization of a mobile WiMAX system. In 2008 he was a visiting researcher at the Institute for Digital Communications, University of Edinburgh, United Kingdom. He joined KTH in 2009. He has participated in several European collaboration projects such as QUASAR, METIS, and METIS-II. His research interests include 5G technologies and architecture, energy-efficient wireless networks, and techno-economics of wireless systems.



Kwang Soon Kim (S'95, M'99, SM'04) was born in Seoul, Korea, on September 20, 1972. He received the B.S. (summa cum laude), M.S.E., and Ph.D. degrees in Electrical Engineering from Korea Advanced Institute of Science and Technology (KAIST), Daejeon, Korea, in February 1994, February 1996, and February 1999, respectively.

From March 1999 to March 2000, he was with the Department of Electrical and Computer Engineering, University of California at San Diego, La Jolla, CA, U.S.A., as a Postdoctoral Researcher. From April 2000 to February 2004, he was with the Mobile Telecommunication Research Laboratory, Electronics and Telecommunication Research Institute, Daejeon, Korea as a Senior Member of Research Staff. Since March 2004, he has been with the Department of Electrical and Electronic Engineering, Yonsei University, Seoul, Korea, now is an Associate Professor.

Prof. Kim is a Senior Member of the IEEE, served as an Editor of the Journal of the Korean Institute of Communications and Information Sciences (KICS) from 2006-2012, as the Editor-in-Chief of the journal of KICS since 2013, as an Editor of the Journal of Communications and Networks (JCN) since 2008, as an Editor of the IEEE Transactions on Wireless Communications since 2009. He was a recipient of the Postdoctoral Fellowship from Korea Science and Engineering Foundation (KOSEF) in 1999. He received the Outstanding Researcher Award from Electronics and Telecommunication Research Institute (ETRI) in 2002, the Jack Neubauer Memorial Award (Best system paper award, IEEE Transactions on Vehicular Technology) from IEEE Vehicular Technology Society in 2008, and LG R&D Award: Industry-Academic Cooperation Prize, LG Electronics, 2013. His research interests are in signal processing, communication theory, information theory, and stochastic geometry applied to wireless heterogeneous cellular networks, wireless local area networks, wireless D2D networks and wireless ad hoc networks.